



**HAL**  
open science

# Temperature-dependence of the UV cross section of dichlorine peroxide in the tail region of the 244 nm signal

Olfa Ferchichi, Najoua Derbel, Thibaud Cours, Alexander Alijah

► **To cite this version:**

Olfa Ferchichi, Najoua Derbel, Thibaud Cours, Alexander Alijah. Temperature-dependence of the UV cross section of dichlorine peroxide in the tail region of the 244 nm signal. *Chemical Physics Letters*, 2021, 764, pp.138261 -. 10.1016/j.cplett.2020.138261 . hal-03493027

**HAL Id: hal-03493027**

**<https://hal.science/hal-03493027>**

Submitted on 2 Jan 2023

**HAL** is a multi-disciplinary open access archive for the deposit and dissemination of scientific research documents, whether they are published or not. The documents may come from teaching and research institutions in France or abroad, or from public or private research centers.

L'archive ouverte pluridisciplinaire **HAL**, est destinée au dépôt et à la diffusion de documents scientifiques de niveau recherche, publiés ou non, émanant des établissements d'enseignement et de recherche français ou étrangers, des laboratoires publics ou privés.



Distributed under a Creative Commons Attribution - NonCommercial 4.0 International License

# Temperature-dependence of the UV cross section of dichlorine peroxide in the tail region of the 244 nm signal

Olfa Ferchichi

*LSAMA, Laboratoire de Spectroscopie Atomique, Moléculaire et Applications, Département of Physics, Faculty of Sciences, University of Tunis - El Manar, 1060 Tunis, Tunisia, and Groupe de Spectrométrie Moléculaire et Atmosphérique, GSMA, UMR CNRS 7331, U.F.R. Sciences Exactes et Naturelles, University of Reims Champagne-Ardenne, 51100 Reims, France*

Najoua Derbel

*LSAMA, Laboratoire de Spectroscopie Atomique, Moléculaire et Applications, Département of Physics, Faculty of Sciences, University of Tunis - El Manar, 1060 Tunis, Tunisia*

Thibaud Cours

*Groupe de Spectrométrie Moléculaire et Atmosphérique, GSMA, UMR CNRS 7331, U.F.R. Sciences Exactes et Naturelles, University of Reims Champagne-Ardenne, 51100 Reims, France*

Alexander Alijah

*Groupe de Spectrométrie Moléculaire et Atmosphérique, GSMA, UMR CNRS 7331, U.F.R. Sciences Exactes et Naturelles, University of Reims Champagne-Ardenne, 51100 Reims, France*

---

## Abstract

We present a physical model that explains the dependence of the UV cross section of ClOOCl on temperature in the actinic wavelength region measured before by J. J. Lin, A. F. Chen and Y. T. Lee [Chemistry - An Asian Journal, **6**, 1664–1678 (2011)]. It was unclear why there are frequency regions in which the cross section decreases with increasing temperature and others in which it increases. This interesting behaviour is now shown to be due to the non-rigidity of the molecule and can be described in terms of the Boltzmann populations of the lowest torsional states and small, non-systematic variations in their absorption cross sections. Combination of these two ingredients produces the non-trivial temperature effect.

**Keywords:** Photoexcitation, UV spectra

---

## 1. Introduction

Dichlorine peroxide is notorious player in the catalytic destruction of the stratospheric ozone layer [1, 2]. Its harmful activities are due to chemical reactions of the radicals produced following absorption of solar UV radiation. The important range of the so-called actinic wavelength region is that with  $\lambda > 300$  nm, as at lower wavelengths ozone and other molecules absorb most of

the UV radiation. It falls in the tail region of a strong signal at  $\lambda \approx 244$  nm.

In their very inspiring review article on the photodissociation of ClOOCl, J. J. Lin, A. F. Chen and Y. T. Lee [3] addressed two issues: the photoabsorption cross section of ClOOCl at wavelengths  $\lambda > 300$  nm and the yields of the possible photo-decomposition channels. A novel experimental setup permitted measurements in the tail region of the  $\lambda = 244$  nm signal, at  $\lambda = 351$  nm, where the absorption cross section is extremely weak. This wavelength has not been accessible in previous measurements. Furthermore, the enhanced experimental resolution and exclusion of impurities in the sample have made it possible to study

---

*Email addresses:* [ferchich.olfa91@gmail.com](mailto:ferchich.olfa91@gmail.com) (Olfa Ferchichi), [najoua.derbel@gmail.com](mailto:najoua.derbel@gmail.com) (Najoua Derbel), [thibaud.cours@univ-reims.fr](mailto:thibaud.cours@univ-reims.fr) (Thibaud Cours), [alexander.aliyah@univ.reims.fr](mailto:alexander.aliyah@univ.reims.fr) (Alexander Alijah)

the temperature-dependence of the cross section in the wavelength range between 248 and 351 nm. The theoretical description of the weak cross section in the tail region is also very difficult, as discussed by Onćák *et al.* [4]. While their computed spectrum is in good agreement with experiment near the centre of the band, their spectrum agrees less well in the tail region. Those authors found that the cross section is sensitive on the molecular geometry which we investigate further in the present letter.

To be sure, temperature effects have been described for other molecules, such as  $\text{Cl}_2$  [5] or ozone and other atmospheric trace gases [6]. In general, at room temperature and even more at the low temperatures of the stratosphere, most molecules are found in their electronic and vibrational ground states, and thus UV cross sections are expected to decrease with increasing temperature as result of depopulation of the vibrational ground state. For hot bands, i.e. bands originating from an excited vibrational state, opposite behaviour is found, see populations in Table 1, and cross sections increase with temperature. This simple, Boltzmann-based model describes most of the behaviour observed for the above-mentioned molecules, except for torsional motion, with a frequency of only about  $112\text{ cm}^{-1}$  or  $3.3\text{ THz}$  (the lowest mode of the rigid ozone molecule has 6 times this frequency,  $\nu = 21\text{ THz}$ ), and several torsional states are noticeably populated even at low temperatures. And then, the simple model cannot justify the change of sign of the slope  $\partial\sigma/\partial T$  with wavelength. It is the aim of the present paper to explain the temperature effect observed in the high-precision measurements by Lin *et al.*

## 2. Theoretical model and results

Dichlorine peroxide is a non-planar molecule with  $C_2$  structure in the electronic ground state  $X^1A$ . The potential energy surface is characterised by two equivalent minima, separated by torsional barriers as shown in Figure 1. As the potential is rather flat around the minima, the frequency of torsional motion is very low and the molecule vibrates with large amplitude.

The properties of this floppy molecule have been investigated recently by the present authors [7]. Only *ab initio* calculations at very high level such as CCSD(T)/aug-cc-pwCVTZ-DK or CCSD(T)-F12/VTZ-F12<sup>1</sup>, coupled to advanced methods for

<sup>1</sup>CCSD(T): coupled cluster theory with all single and double excitations and perturbative triples corrections. CCSD(T)-F12: explicitly correlated CCSD(T). Basis sets: aug-cc-pwCVTZ-DK: relativistic

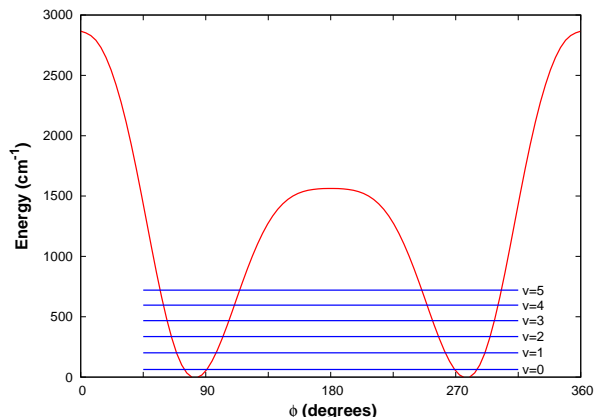


Figure 1: Torsional potential, computed at the CCSD(T)-F12/VTZ-F12 level, and lowest torsional states without tunneling splitting. The *trans* barrier is located at  $\phi = 180^\circ$ , the *cis* barrier at  $\phi = 0^\circ$ .

the computation of the vibrational modes, such as vibrational VMP2 (second order vibrational Møller-Plesset perturbation theory) are able to provide frequencies in very good agreement with experiment [8], in particular for the torsional mode (theory:  $\tilde{\nu}_1 = 111.21\text{ cm}^{-1}$  and  $112.20\text{ cm}^{-1}$ , respectively, experiment:  $127 \pm 20\text{ cm}^{-1}$ , force-field value:  $114\text{ cm}^{-1}$ ). The next higher modes have VMP2 frequencies  $\tilde{\nu}_{2,\dots,6} = 325.47, 436.83, 576.69, 654.80, 750.93\text{ cm}^{-1}$ , while the experimental values obtained in an argon matrix are  $\tilde{\nu}_{2,\dots,6} = -, 418.5, 543, 647.67, 753.97\text{ cm}^{-1}$  for the main isotopologue.

We have developed a one-dimensional model to investigate the temperature-dependence of the UV cross section in the tail region. In this model, only the torsional motion is taken into account explicitly. An effective torsional potential was obtained at the CCSD(T)-F12/VTZ-F12 level. At each torsional angle  $\phi$ , the remaining coordinates were optimized without imposing any symmetry conditions, they are denoted as  $\mathbf{x}(\phi)$ . This one-dimensional potential was then used to compute the torsional energy levels and wavefunctions. As in a previous publication [9], the internal coordinates were transformed to local orthogonal coordinates [10], in which vibrational modes are approximately decoupled. This transformation generates an effective reduced mass which is no longer constant but a function of the transformed torsional angle. The torsional Schrödinger equation was integrated with our own Numerov code, within half of the full interval, i.e.  $180^\circ \leq \phi \leq 360^\circ$ ,

Douglas-Kroll augmented correlation-consistent polarized weighted core-valence triple-zeta. VTZ-F12: correlation-consistent polarized valence triple-zeta for explicitly correlated methods

as tunneling splitting can be neglected. The computed torsional energies are collected in Table 1, as well as the Boltzmann weights of the corresponding states at four temperatures. For each state, with energy  $E_\nu$ , the full nuclear configuration,  $\mathbf{x}(\phi)$ , was recovered from the averaged  $\phi$ -angle,  $\langle\phi\rangle_\nu$ . We noticed that while the vibrational average  $\langle\phi\rangle_\nu$  increases from  $83^\circ$  to  $93^\circ$  as  $\nu$  is increased, the averaged values of the remaining internal coordinates are practically constant.

These configurations were then used as initial configurations in a state-dependent simulation of the UV spectrum using the Newton-X code [11] and TD-DFT theory. The combination of the M05-2X functional and the AVTZ basis has shown to be accurate in our recent publication [7] and has therefore been employed also in the present work. The photoabsorption cross section for excitation from a torsional states  $\nu$  is computed as

$$\sigma_\nu(\lambda) = \frac{\pi e^2}{2mc\epsilon_0} \sum_{l \neq i}^{N_{fs}} \left[ \frac{1}{N_p} \sum_k^{N_p} f_{il}(\mathbf{x}_k) g(E - \Delta E_{il}(\mathbf{x}_k), \delta) \right] \quad (1)$$

where  $e$  is the elementary charge,  $m$  the electron mass,  $c$  the speed of light and  $\epsilon_0$  the vacuum permittivity.  $E = hc/\lambda$  is the radiation energy. The outer sum of the above equation runs over excited electronic states,  $l$ .  $f_{il}$  is the oscillator strength for transitions between the initial electronic state  $i$  and the final state  $l$ , while  $\Delta E_{il}$  denotes the transition energy. The inner sum samples the nuclear configurations,  $\mathbf{x}_k$ . These nuclear configurations are obtained as deviations from a reference configuration, which we have chosen as the configuration with the largest amplitude of the wavefunction of the initial torsional state  $\nu$ .  $g$  is a Gaussian lineshape function with a broadening of  $\delta = 0.06\text{eV}$ , which is large enough to remove statistical noise, as described in detail by Barbatti *et al.* [12]. The choice of initial torsional states was made according to their Boltzmann populations. For the temperature range of the experiment,  $160\text{ K} \leq T \leq 260\text{ K}$ , the population drops below 10% above  $\nu = 5$ , see Table 1. We have thus restricted our analysis to states with  $\nu \leq 5$ . Figure 2 shows the computed UV spectra,  $\sigma_\nu(\lambda)$ , in the tail region for the six initial torsional states. The cross section clearly depends on the initial state. At  $\lambda \approx 248\text{ nm}$ , we find  $\sigma_{\nu=1} \approx \sigma_{\nu=2} < \sigma_{\nu=0}$ , while around  $\lambda \approx 277\text{ nm}$  the cross section is about the same for the six torsional states. In the tail region, at  $\lambda \gtrsim 280\text{ nm}$ , the cross section by and large increases with the torsional quantum number  $\nu$ .

As many as four excited electronic states, all repulsive, are accessible in the wavelength region of interest. The excited states come as nearly degenerate pairs [13] ( $1^1B/2^1A$ ) and ( $3^1A/4^1B$ ). The threshold wavelengths for vertical excitation as obtained with the

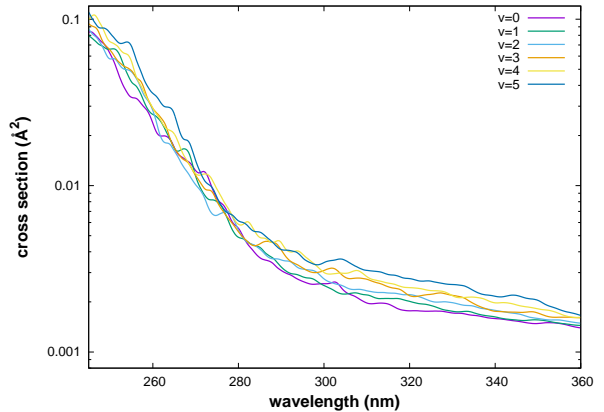


Figure 2: Unweighted theoretical cross sections for the lowest torsional states.

present method are  $\lambda_{1,2} \approx 354\text{ nm}$  and  $\lambda_{3,4} \approx 260\text{ nm}$ . These values apply for the torsional state  $\nu = 5$ . There is a small variation of up to 4 nm with respect to  $\nu$ .

The oscillator strength to the second excited state is almost zero, which means that the transitions for  $\lambda > \lambda_{3,4}$  all reach the first excited state. The temperature dependence of the cross section is therefore free from possible complications due to overlapping continua.

To simulate the temperature-dependent UV spectra, the individual spectra of Figure 2 have been superimposed, weighted with the Boltzmann factors  $w_\nu$ , reported in Table 1.

$$\sigma(\lambda; T) = \sum_\nu w_\nu(T) \sigma_\nu(\lambda) \quad (2)$$

Figure 3 shows these spectra, together with data from the Lin group and the recommended cross section from the latest evaluation report of the Jet Propulsion Laboratory [14]. Their latter data over most part of the relevant tail region appear to be represented by a declining exponential, which leads to too small cross sections for  $\lambda > 340\text{ nm}$ . It is important to recall that the cross sections in the tail region are extremely small, only about 1% of its value at the maximum of the peak, and extremely difficult to describe by whatever means. We note in particular that the vertical excitation energies alone are not sufficient to understand the characteristics of the spectrum. The position of the maximum of the peak does not coincide with any of the vertical excitation energies, and neither does the intensity of the peak coincide with any of the individual cross sections, as we have found in a recent publication [7]. Several excited states contribute to the signal. It is therefore difficult to judge the performance of a particular theoretical method solely on the basis of positions and oscillator strengths

Table 1: Energies and Boltzmann populations, at four temperatures, of the lowest torsional states. The potential was computed at the CCSD(T)-F12/VTZ-F12 level of theory.

$\nu$	$E_\nu$ (cm <sup>-1</sup> )	population, $w_\nu$			
		$T = 160$ K	$T = 200$ K	$T = 250$ K	$T = 260$ K
0	63.43	0.707	0.624	0.540	0.526
1	201.36	0.205	0.231	0.244	0.245
2	336.27	0.061	0.088	0.112	0.116
3	467.94	0.019	0.034	0.053	0.056
4	596.09	0.006	0.014	0.025	0.028
5	720.50	0.002	0.006	0.012	0.014
6	840.99	0.001	0.002	0.006	0.007

of electronic transitions. These vary within a certain margin, as can be seen particularly well in the profound analysis presented by Ončák and coworkers [4]. The near-degeneracy of the electronic states  $3^1A$  and  $4^1B$  is not maintained for most multi-reference methods. This has no implication for the present work since these states are not energetically accessible in the tail region. However, as observed by those authors, intensities depend to quite some extent on the nuclear configurations. The sampling procedure of these configurations is arguably the factor that influences most the computed spectrum in the long-wavelength tail of the peak. Our sampling procedure and “manual” Boltzmann weighting, Eq. (2), is different from the procedures employed by other workers [4, 12].

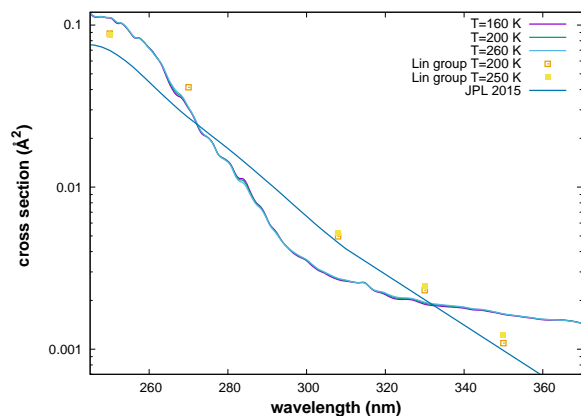


Figure 3:  $T$ -dependence of the UV spectrum.

The fine temperature effects of the cross sections are hardly noticeable even on the logarithmic scale applied in Figure 3. In Figure 4 we have thus redrawn our results in the way chosen by Lin *et al.* [3]. Those authors, in their Figure 5, show, for four wavelengths, the cross sections normalised with respect to the cross sections at  $T = 200$  K, as function of the tempera-

ture for  $160 \text{ K} \leq T \leq 260 \text{ K}$ . At the wavelength  $\lambda = 248 \text{ nm}$ , the cross section declines as the temperature is increased. This can be understood from the above discussion, which shows that at  $248 \text{ nm}$  the  $\nu = 0$  contribution is larger than the  $\nu = 1$  and  $\nu = 2$  contributions. Hence, as the temperature increases, the cross section decreases since the  $\nu = 1$  and  $\nu = 2$  states become more strongly populated. At about  $\lambda = 277 \text{ nm}$ , there is a crossing as the state-dependent cross sections  $\sigma_\nu$  are almost the same. At larger wavelengths we have approximately  $\sigma_\nu \geq \sigma_{\nu'}$  for  $\nu > \nu'$ , so that the cross section increases with temperature, which can indeed be seen in the figures. Only one single point in the  $351 \text{ nm}$  plot is outside the error bars. Though the agreement is not 100%, the physical phenomenon is described correctly.

A general impression of the temperature behaviour over the full tail region can be obtained from Figure 5, which shows the ratio of the cross sections at temperatures  $T = 160 \text{ K}$  and  $T = 260 \text{ K}$ . It is an estimate of the average slope  $\partial\sigma(\lambda; T)/\partial T$  within the temperature interval. Regions of positive and negative slopes can clearly be distinguished. A small change in the wavelength may alter the temperature behaviour qualitatively.

A number of interesting questions arise, for example how isotopic substitution would alter the temperature dependence of the absorption cross section or whether unusual temperature effects can be observed in other peroxides or related compounds such as persulfides. Isotopic substitution of  $^{35}\text{Cl}$  by  $^{37}\text{Cl}$  is not expected to have a sizeable effect on the temperature dependence as such substitution reduces the torsional frequency by about  $1 \text{ cm}^{-1}$  only. The lighter difluorine peroxide has a torsional frequency of about  $200 \text{ cm}^{-1}$ . Therefore a regular  $T$ -dependence of the UV excitation spectrum is expected, i.e. a decrease of the cross section with increasing temperature, which is indeed the case. Two years ago, we have studied the unusual structure and spectroscopic properties of this molecule [15], includ-

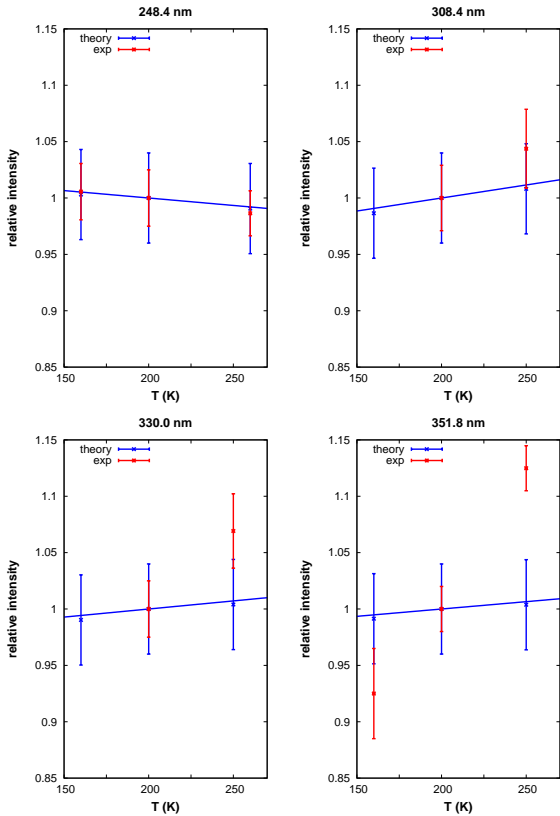


Figure 4:  $T$ -dependence of the cross section as function of the wavelength. Shown are the relative values  $\sigma(T)/\sigma(T = 200 \text{ K})$ , just as in Ref. [3].

ing the UV spectrum in the range  $\lambda > 200 \text{ nm}$  which has been measured experimentally. It corresponds to the long-wavelength tail of a signal at  $\lambda = 155 \text{ nm}$ . The cross section of the experimental spectrum recorded at  $T = 77 \text{ K}$  is consistently higher than the JPL-recommended cross-section for the  $193 \text{ K} < T < 298 \text{ K}$  range [16]. Our computed spectrum, not  $T$ -resolved, lies inbetween. The much heavier dibromine peroxide has a lower torsional frequency than dichlorine peroxide, and thus more torsional states may be required in the simulation. Some non-trivial temperature effect is expected, but is difficult to predict. In contrast to CIOOCI, the potential energy surfaces of the excited electronic states of BrOOBr have local minima [17], and UV excitation from the electronic ground state surface might produce pre-dissociative complexes. Computation of Franck-Condon factors is then required for a realistic description of the UV cross sections, which is not included in the present model. In conclusion, complex temperature effects are expected to be found in molecules with low torsional frequencies, but their

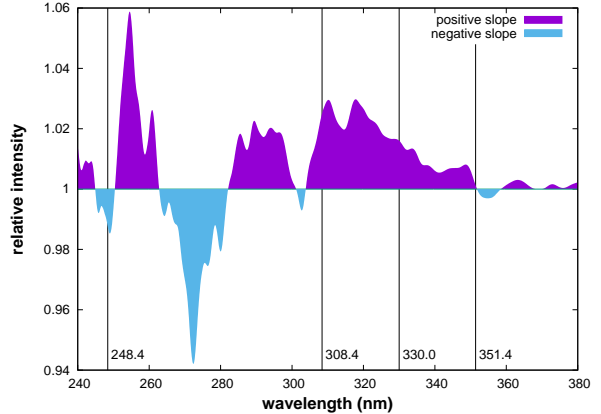


Figure 5:  $T$ -dependence of the cross section as function of the wavelength in the tail region. Relative values presented are  $\sigma(T = 160 \text{ K})/\sigma(T = 260 \text{ K})$ . Regions with positive and negative  $T$ -dependences can be distinguished.

analysis requires for each individual case the set up of an adequate model.

### 3. Conclusions

Almost ten years ago Lin, Chen and Lee [3] published UV absorption cross sections with enhanced accuracy and precision at four wavelengths, including three in the tail region of the 244 nm peak. Their results at 351 nm are the first to be obtained at such a wavelength and should contribute to define the long-range cross section data with much higher precision. They noticed a weak temperature dependence that till today has remained unaccounted for. In the present work we have elucidated this effect and shown that it is a consequence of the floppiness of the dichlorine peroxide molecule. The torsional angle changes largely as the torsional mode gets excited, to within ten degrees considering the experimental temperature range. The vibrationally averaged molecular structure is altered substantially which impacts the cross sections. Cross sections of transitions starting from particular torsional states are not simply running parallel but show several crossings within the considered wavelength region. When these cross sections are Boltzmann-weighted and superimposed, a non-trivial temperature effect is produced which describes well the experimental findings. We note in particular that the signs of the temperature slopes are correct, which is a remarkable result given the extremely weak cross sections. Fine-tuning through inclusion of the symmetric and antisymmetric bending modes would likely lead to a better agreement. But it

would not alter in any way the principal conclusion of our work.

## Acknowledgments

The authors thank Prof. Mario Barbatti for his valuable advice on the use of Newton-X. They gratefully acknowledge financial support from the “PHC Utique” programme of the French Ministry of Foreign Affairs and Ministry of Higher Education and Research and the Tunisian Ministry of Higher Education and Scientific Research, project number 18G1302, and computer time provided by the ROMEO HPC Center at the University of Reims Champagne-Ardenne and by CRIANN (Centre des Ressources Informatiques et Applications Numériques de Normandie).

## References

- [1] M. J. Molina, F. S. Rowland, Stratospheric sink for chlorofluoromethanes: chlorine atom-catalysed destruction of ozone, *Nature* 249 (5460) (1974) 810–812.  
URL <https://www.nature.com/articles/249810a0>
- [2] L. T. Molina, M. J. Molina, Production of chlorine oxide ( $\text{Cl}_2\text{O}_2$ ) from the self-reaction of the chlorine oxide ( $\text{ClO}$ ) radical, *The Journal of Physical Chemistry* 91 (2) (1987) 433–436. arXiv:<https://doi.org/10.1021/j100286a035>, doi:10.1021/j100286a035.  
URL <https://doi.org/10.1021/j100286a035>
- [3] J. J. Lin, A. F. Chen, Y. T. Lee, UV photolysis of  $\text{ClOOCl}$  and the ozone hole, *Chemistry - An Asian Journal* 6 (7) (2011) 1664–1678. arXiv:<https://onlinelibrary.wiley.com/doi/pdf/10.1002/asia.201100151>, doi:10.1002/asia.201100151.  
URL <https://onlinelibrary.wiley.com/doi/abs/10.1002/asia.201100151>
- [4] M. Ončák, L. Šišťík, P. Slavíček, Can theory quantitatively model stratospheric photolysis? Ab initio estimate of absolute absorption cross sections of  $\text{ClOOCl}$ , *The Journal of Chemical Physics* 133 (17) (2010) 174303. arXiv:<https://doi.org/10.1063/1.3499599>, doi:10.1063/1.3499599.  
URL <https://doi.org/10.1063/1.3499599>
- [5] I. A. K. Young, C. Murray, C. M. Blaum, R. A. Cox, R. L. Jones, F. D. Pope, Temperature dependent structured absorption spectra of molecular chlorine, *Phys. Chem. Chem. Phys.* 13 (2011) 15318–15325. doi:10.1039/C1CP21337G.  
URL <http://dx.doi.org/10.1039/C1CP21337G>
- [6] K. Bogumil, J. Orphal, J. P. Burrows, Temperature dependent absorption cross sections of  $\text{O}_3$ ,  $\text{NO}_2$ , and other atmospheric trace gases measured with the SCIAMACHY spectrometer, in: *Proceedings of the ERS-ENVISAT Symposium, ESA-ESTEC, 2000*.
- [7] O. Ferchichi, N. Derbel, T. Cours, A. Alijah, Dichlorine peroxide ( $\text{ClOOCl}$ ), chloryl chloride ( $\text{ClCl(O)O}$ ) and chlorine chlorite ( $\text{ClOClO}$ ): very accurate ab initio structures and actinic degradation, *Phys. Chem. Chem. Phys.* 22 (2020) 4059–4071. doi:10.1039/C9CP06875A.  
URL <http://dx.doi.org/10.1039/C9CP06875A>
- [8] J. Jacobs, M. Kronberg, H. S. P. Mueller, H. Willner, An experimental study on the photochemistry and vibrational spectroscopy of three isomers of  $\text{Cl}_2\text{O}_2$  isolated in cryogenic matrices, *Journal of the American Chemical Society* 116 (3) (1994) 1106–1114. arXiv:<https://doi.org/10.1021/ja00082a038>, doi:10.1021/ja00082a038.  
URL <https://doi.org/10.1021/ja00082a038>
- [9] O. Ferchichi, N. Derbel, N.-E. Jaidane, T. Cours, A. Alijah, The gas-phase structure of dimethyl peroxide, *Physical Chemistry Chemical Physics* 19 (2017) 21500–21506. doi:10.1039/C7CP03134C.  
URL <http://dx.doi.org/10.1039/C7CP03134C>
- [10] G. S. Maciel, A. C. P. Bitencourt, M. Ragni, V. Aquilanti, Studies of the dynamics around the O–O bond: Orthogonal local modes of hydrogen peroxide, *Chemical Physics Letters* 432 (4–6) (2006) 383–390. doi:<http://dx.doi.org/10.1016/j.cplett.2006.10.073>.  
URL <http://www.sciencedirect.com/science/article/pii/S0009261406015739>
- [11] M. Barbatti, M. Ruckebauer, F. Plasser, J. Pittner, G. Granucci, M. Persico, H. Lischka, Newton-X: a surface-hopping program for nonadiabatic molecular dynamics, *Wiley Interdisciplinary Reviews: Computational Molecular Science* 4 (1) (2014) 26–33, 00069. doi:10.1002/wcms.1158.  
URL <http://onlinelibrary.wiley.com/doi/10.1002/wcms.1158/abstract>
- [12] M. Barbatti, A. J. A. Aquino, H. Lischka, The UV absorption of nucleobases: semi-classical ab initio spectra simulations, *Phys. Chem. Chem. Phys.* 12 (2010) 4959–4967. doi:10.1039/B924956G.  
URL <http://dx.doi.org/10.1039/B924956G>
- [13] K. A. Peterson, J. S. Francisco, Does chlorine peroxide absorb below 250 nm?, *The Journal of Chemical Physics* 121 (6) (2004) 2611–2616. arXiv:<https://aip.scitation.org/doi/pdf/10.1063/1.1766012>, doi:10.1063/1.1766012.  
URL <https://aip.scitation.org/doi/abs/10.1063/1.1766012>
- [14] J. B. Burkholder, S. P. Sander, J. P. D. Abbatt, J. R. Barker, R. E. Huie, C. E. Kolb, M. J. Kurylo, V. L. Orkin, D. M. Wilmouth, P. H. Wine, Chemical kinetics and photochemical data for use in atmospheric studies: evaluation number 18, Tech. rep., Pasadena, CA: Jet Propulsion Laboratory, National Aeronautics and Space Administration (2015).  
URL <https://jpldataeval.jpl.nasa.gov/download.html>
- [15] O. Ferchichi, A. Alijah, T. Cours, N.-E. Jaidane, N. Derbel, Accurate theoretical characterization of dioxygen difluoride: a problem resolved, *Phys. Chem. Chem. Phys.* 20 (2018) 11826–11832. doi:10.1039/C7CP08659H.  
URL <http://dx.doi.org/10.1039/C7CP08659H>
- [16] H. Keller-Rudek, G. K. Moortgat, R. Sander, R. Sörensen, The MPI-Mainz UV/VIS spectral atlas of gaseous molecules of atmospheric interest, *Earth System Science Data* 5 (2) (2013) 365–373.  
URL <http://www.uv-vis-spectral-atlas-mainz.org>
- [17] Y. Li, C. K. Vo, Computational studies on the ground and excited states of  $\text{BrOOBr}$ , *The Journal of Chemical Physics* 124 (20) (2006) 204309. arXiv:<https://doi.org/10.1063/1.2197831>, doi:10.1063/1.2197831.  
URL <https://doi.org/10.1063/1.2197831>